remote sensing

MDPI

Article

Spatio-Temporal Heterogeneous Impacts of the Drivers of NO_2 Pollution in Chinese Cities: Based on Satellite Observation Data

Yuanzheng Cui [1,2], Hui Zha [1], Yunxiao Dang [3], Lefeng Qiu [3], Qingqing He [4] and Lei Jiang [5,*]

[1] College of Hydrology and Water Resources, Hohai University, Nanjing 210098, China; ryancyz@hhu.edu.cn (Y.C.); geozhahui@hhu.edu.cn (H.Z.)
[2] Key Laboratory of Watershed Geographic Sciences, Nanjing Institute of Geography and Limnology, The Chinese Academy of Sciences, Nanjing 210008, China
[3] Institute of Land and Urban-Rural Development, Zhejiang University of Finance and Economics, Hangzhou 310018, China; dangyx@zufe.edu.cn (Y.D.); qiulefeng@zufe.edu.cn (L.Q.)
[4] School of Resources and Environmental Engineering, Wuhan University of Technology, Wuhan 430070, China; qqhe@whut.edu.cn
[5] School of Geography and Remote Sensing, Guangzhou University, Guangzhou 510006, China
* Correspondence: jianglei@gzhu.edu.cn; Tel.: +86-158-7235-1777

Abstract: Rapid urbanization in China has led to an increasing problem of atmospheric nitrogen dioxide (NO_2) pollution, which negatively impacts urban ecology and public health. Nitrogen dioxide is an important atmospheric pollutant, and quantitative spatio-temporal analysis and influencing factor analysis of Chinese cities can help improve urban air pollution. In this study, the spatio-temporal analysis methods were used to explore the variations of NO_2 pollution in Chinese cities from 2005 to 2020. The findings are as follows. In more than half of Chinese cities, NO_2 levels remarkably decreased between 2005 and 2020. The effective NO_2 reduction strategies contributed to the significant NO_2 reduction during the 13th Five-Year Plan (2016–2020). Moreover, we found that the pandemic of COVID-19 alleviated NO_2 pollution in China since it reduced the traffic, industrial, and living activities. The NO_2 pollution in Chinese cities was found highly spatially clustered. The geographically and temporally weighted regression model was used to analyze the spatio-temporal heterogeneity of NO_2 pollution influencing factors in Chinese cities, including natural meteorological and socio-economic factors. The results showed that the GDPPC, population densities, and ambient air pressure were positively correlated with NO_2 pollution. In contrast, the ratio of the tertiary to the secondary industry, temperature, wind speed, and relative humidity negatively impacted the NO_2 pollution level. The findings of this research contribute to the improvement of urban air quality, stimulating the achievements of the sustainable development goals of Chinese cities.

Keywords: NO_2 pollution; satellite observation data; spatio-temporal heterogeneity; Chinese cities; natural meteorological factors; socio-economic factors; urban air quality

check for updates

Citation: Cui, Y.; Zha, H.; Dang, Y.; Qiu, L.; He, Q.; Jiang, L. Spatio-Temporal Heterogeneous Impacts of the Drivers of NO_2 Pollution in Chinese Cities: Based on Satellite Observation Data. *Remote Sens.* **2022**, *14*, 3487. https://doi.org/10.3390/rs14143487

Academic Editor: Carmine Serio

Received: 18 June 2022
Accepted: 19 July 2022
Published: 21 July 2022

1. Introduction

In recent years, the use of tremendous amounts of fossil energy in Chinese cities has resulted in nitrogen oxide pollutants into the atmosphere, severely worsening the air quality. Nitrogen oxides (NO_x) are made up of two compounds: nitrogen monoxide (NO) and nitrogen dioxide (NO_2) [1]. Notably, NO_2 has posed a huge threat to the air quality of Chinese cities. As a result, it has become a significant pollutant in urban air quality monitoring systems [2].

NO_2 has had the fastest concentration growth rate in China over the last two decades [3]. Numerous studies have demonstrated that long-term exposure to high NO_2 concentrations increases mortality from respiratory and cardiovascular diseases [4]. Additionally, NO_2 is a significant contributor to acid rain and photochemical smog [3]. Most significantly, NO_2 takes part in the formation of ozone and aerosol, affecting the local climate change [5].

The Chinese government's National Air Pollution Prevention and Control Joint Center has conducted a synergistic treatment of $PM_{2.5}$ and ozone [6]. In addition, in 2015, the United Nations established 17 Sustainable Development Goals (SDGs) as a plan of action to achieve global peace and prosperity by 2030 [7]. The mitigation of NO_2 pollution is closely related to the mapping of hazardous chemicals and pollutants in the air, water, and soil in SDG Target 3 "good health and well-being", mapping of air quality in SDG Target 11 "sustainable cities and communities", and the environmental variables for climate change models in SDG Target "climate action" [8,9]. Therefore, NO_2 has received increased attention from researchers and global governments. China, as the biggest developing country, also has suffered from NO_2 pollution for a long time. Hence, it is necessary to analyze the spatio-temporal distribution of NO_2 pollution in China and explore its influencing factors.

NO_2 pollution is primarily measured based on the ground platform. However, we discovered that the ground observations over China were unevenly distributed within the short period of historical time series (only available after 2013). On the other hand, satellite remote sensing observation data have the advantages of broad spatial coverage, a long observation period, and spatial continuity [10,11]. Therefore, the tropospheric NO_2 vertical column densities (VCDs) data retrieved by the Ozone Monitoring Instrument (OMI) are widely applied to detect the long-term variations in NO_2 pollution over China and investigate the drivers from a spatio-temporal perspective [1,3,5].

During the last two decades, many researchers have used satellite observation technologies to study the various factors influencing NO_2 pollution over China [12]. Since industrial, transportation, and residential emissions are all anthropogenic sources of NO_x emissions [13], fluctuations in NO_2 concentrations are highly correlated with human activities [14]. It has been found that civil vehicles, electricity consumption, total population, built-up areas, and coal use are closely correlated with NO_2 pollution levels [12]. Wang et al. [15] analyzed the spatial and temporal distribution of NO_2 columns over China using the simple linear regression model based on OMI satellite observations. The association between changes in NO_2 pollution and urbanization in China was also conducted [3,16]. Bucsela et al. [17] used satellite measurements to examine the impacts of income and urban spatial form on urban NO_2 levels. Since air pollution is a regional problem, the traditional linear regression method cannot solve the spatial autocorrelation problem of air pollution. However, spatial econometric models can effectively address the complex spatial interactions and spatial dependence factors in regression models. The link between NO_2 pollution and its natural and socio-economic factors in Chinese cities was quantified by incorporating spatial effects in an extended STIRPAT model (stochastic impacts by regression on population, affluence, and technology) [12]. Moreover, socio-economic or public health events that significantly influence human activities can affect local NO_2 pollution levels, such as regional economic recessions [18,19], the 2008 Beijing Olympic Games [20], the 2016 G20 Hangzhou Summit [21], and the COVID pandemic incidents [2,22–25].

The studies mentioned above drew fruitful conclusions but neglected the variability of influencing factors of NO_2 pollution under different spatial and temporal conditions. Additionally, NO_x emissions in eastern China grew fast between 2000 and 2011 and began to fall steadily [26,27]. Governments recently established a regional coordinated development strategy, in which economically underdeveloped regions in central and western China were encouraged to absorb the energy-intensive industry shifted from the eastern coastal regions [28]. Since the 12th Five-Year Plan (2011–2015), some cities in central China and western China remarkably increased their NO_x emissions [3]. It has been evidenced that spatially varying socio-economic conditions and natural geographic factors contribute to varying levels of NO_2 pollution at the city level [12]. In other words, these existing studies disclosed the average impacts of the drivers of NO_2 pollution over China, and they paid little attention to the spatio-temporal variations of the drivers from one city to another, which could mask important information on NO_2 pollution prevention and control based on the characteristics of Chinese cities.

Hence, our study aims to fill this gap using a novel geographically and temporally weighted regression (GTWR) approach proposed by Huang et al. [29] to test the spatio-temporal heterogeneity of the influencing factors of NO_2 pollution in each prefecture-level city. Huang et al. [29] incorporated both spatial and temporal characteristics into a regression model on the basis of the classical geographically weighted regression (GWR) approach and proposed the effective construction method of the spatio-temporal distance. In recent years, the GTWR model has been widely used in many studies to explore the heterogeneous relationships between independent and dependent variables in time and space, such as the relationship between carbon emissions and urbanization [30], air pollutants and natural geographical conditions [31,32], and ecosystem services and human factors [33].

This study first analyzed the spatial and temporal variations of NO_2 pollution over China from 2005 to 2020 using satellite observations data. Then, the GTWR model was applied to explore the influencing factors on the NO_2 pollution at the city level over China. Finally, the relationship between NO_2 pollution and both metrological and socio-economic variables was investigated and quantified. The findings of this study may provide both potential solutions for China's urban air pollution prevention and control and scientific support for achieving sustainable development goals for China.

2. Materials and Methods

2.1. Data Description

The tropospheric NO_2 VCDs were retrieved by the Ozone Monitoring Instrument onboard the EOS-Aura satellite [34]. The satellite, launched in September 2004, is in a sun-synchronous orbit at 705 km altitude with a 99 min time period. It has the OMI pixel size of 13×24 km^2 at nadir in the global mode and 13×12 km^2 in the zoom mode, with a local passage time of approximately 13:40 [10]. We used the Royal Netherlands Meteorological Institute's (KNMI) monthly QA4ECV NO_2 long-term dataset (version 1.1) in this study (https://www.temis.nl/airpollution/no2col/no2regioomimonth_qa.php, accessed on 16 March 2022). The QA4ECV tropospheric NO_2 VCDs product has a spatial resolution of $0.125° \times 0.125°$. The updated NO_2 retrieval algorithms were referred to Boersma, Eskes, Dirksen, van der A, Veefkind, Stammes, Huijnen, Kleipool, Sneep, Claas, Leitão, Richter, Zhou, and Brunner [34] and Boersma et al. [35]. The monthly data have an uncertainty of approximately 10% but range from 15% to 30% in contaminated places [35]. We further removed the data with row anomalies and cloud radiance fractions of more than 50%. Then, the monthly gridded composite of tropospheric NO_2 VCDs was averaged into the annual NO_2 VCDs gridded dataset.

The independent variables in the GTWR model are introduced and processed as follows. The ground-based meteorological variables, including temperature (temp), wind speed (WS), ambient air pressure near the ground (Pres), and relative humidity (Humi), were obtained from the National Meteorological Information Center of China Meteorological Administration (http://data.cma.cn/, accessed on 16 March 2022). Given the daily station monitoring data, we applied an inverse distance–weighted (IDW) interpolated method to interpolate into grid data with the spatial resolution of $0.125° \times 0.125°$, keeping the consistency with the spatial resolution of the QA4ECV tropospheric NO_2 VCDs product. The daily dataset was then processed into an annual mean dataset. Meanwhile, the yearly socio-economic variables and indicators of Chinese cities from 2005 to 2019, including foreign direct investment (FDI), population density (PD), gross domestic product per capita (GDPPC), and the ratio of the tertiary to the secondary industry (TSRatio), were obtained from the China Statistical Yearbooks and the China City Statistical Yearbooks. In addition, the tropospheric NO_2 and meteorological parameters at the prefectural level were retrieved according to China's administrative boundary vector data (http://www.resdc.cn/, accessed on 16 March 2022) by using ArcGIS 10.8 software.

It should be noted that although the data for NO_2 VCDs of prefecture-level cities are extracted, due to the data unavailability of the explanatory variables for some cities, the sample size in the regression analysis is restricted to 271 prefecture-level cities. The descriptive statistics of the variables involved in the regression models (standard deviation (S.D.), mean, median, minimum (Min), and maximum (Max)) are summarized in Table 1.

Table 1. Descriptive statistics for variables included in this study.

Variable	S.D.	Mean	Median	Min	Max
$LnNO_2$	0.796	6.197	6.149	4.097	8.111
LnFDI	4.008	15.580	16.303	0.000	24.569
LnPD	0.881	5.795	5.929	1.547	9.984
LnGDPPC	0.855	10.295	10.269	6.638	13.185
LnTSRatio	0.495	0.886	0.787	0.094	9.482
LnTemp	0.138	2.823	2.808	2.301	3.256
LnWS	0.231	0.725	0.741	0.085	1.563
LnPres	2.974	5.320	6.887	−0.925	6.924
LnHumi	0.146	−0.384	−0.333	−0.983	−0.136

2.2. Methodology

We note that NO_2 VCDs in adjacent cities tend to be similar. In other words, NO_2 pollution may exhibit spatial autocorrelation. Hence, global Moran's I is introduced to test if there is spatial dependence for NO_2 VCDs of Chinese cities. It is as follows:

$$I = \frac{n}{S_0} \frac{\sum_{i=1}^{n} \sum_{j=1}^{n} W_{ij} \left(Y_i - \overline{Y}\right) \left(Y_j - \overline{Y}\right)}{\sum_{i=1}^{n} \left(Y_i - \overline{Y}\right)^2} \quad (1)$$

where $S_0 = \sum_{i=1}^{n} \sum_{j=1}^{n} W_{ij}$. Y_i, Y_j, and $\overline{Y}$ are the NO_2 VCDs of city i, j, and are the average values of NO_2 VCDs of all samples. W_{ij} denotes a spatial weights matrix, which describes the spatial arrangement of these cities. n is the number of all samples.

When the global Moran's I is significant and positive, it indicates that NO_2 pollution of one city is similar to that of its neighbors, namely a spatial clustering. When global Moran's I is significant and negative, it shows that NO_2 pollution is spatially dispersed. When global Moran's I equals zero, NO_2 pollution may be randomly distributed in space.

Anselin [36] proposed a local Moran's I, called the local indicator of spatial association (LISA), to test whether similar or dissimilar observations are clustered together in a local area. The local Moran's I value of each city can be calculated as follows:

$$I_i = \frac{(x_i - \overline{x})}{S^2} \sum_{j \neq i} w_{ij} (x_i - \overline{x}) \quad (2)$$

where w_{ij} is also the spatial weights matrix; x_i is the attribute of city I; and $\overline{x}$ is the mean value of the attributes. $S^2 = \frac{1}{n} \sum_i (x_i - \overline{x})^2$ is the variance of the attributes.

In this study, to measure the importance of the explanatory factors affecting NO_2 VCDs, the independent variables can be standardized as follows:

$$X'_k = \frac{X_k - X_{k\_min}}{X_{k\_max} - X_{k\_min}} \times 100\% \quad (3)$$

where X'_k is the standardized independent variable k. X_k is the original independent variable k. X_{k_min} and X_{k_max} are the minimum and maximum values of the independent variable k, respectively.

We use the GTWR model to quantify the spatio-temporal heterogeneous impacts of different independent variables on NO_2 VCDs changes in Chinese cities. Compared with the cross-sectional data used in the traditional GWR model, the GTWR model incorporates temporal variations into the GWR model. In this study, the ordinary least squares (OLS), GWR, temporally weighted regression (TWR), and GTWR models are all conducted for completeness and comparison on the ArcGIS 10.8 software. The GTWR model can be expressed as follows:

$$Y_i = \beta_0(u_i, v_i, t_i) + \sum_n \beta_n(u_i, v_i, t_i)X_{in} + \varepsilon_i \tag{4}$$

where (u_i, v_i, t_i) denotes city i at location (u_i, v_i) and year t_i; $\beta_0(u_i, v_i, t_i)$ is an intercept, $\beta_n(u_i, v_i, t_i)$ is the unknown coefficient of influencing factors to be estimated, including meteorological conditions and socio-economic factors; ε_i denotes a random error.

Therefore, the coefficients $\beta_n(u_i, v_i, t_i)$ are estimated by the least-squares method. The estimator reads below:

$$\hat{\beta}_n(u_i, v_i, t_i) = \left[X^T W(u_i, v_i, t_i)X\right]^{-1} X^T W(u_i, v_i, t_i)Y \tag{5}$$

where $W(u_i, v_i, t_i) = diag(a_{i1}, a_{i2}, \ldots, a_{ik})$, and k is the number of the explanatory variables. The GTWR model is essentially determined by the ability of the kernel function in the weight matrix to solve for both the temporal non-smoothness and spatial non-smoothness. The weight matrix is computed by the Euclidean distance and Gaussian distance-decay-based functions, as described in Wu et al. [37]. The weight scheme is generated by a bandwidth parameter h [38], and the schematic diagram of the spatio-temporal distance d_{ij}^{ST} between cities i and j is shown in Figure 1 and represented as follows:

$$\left(d_{ij}^{ST}\right)^2 = \left(u_i - u_j\right)^2 + \left(v_i - v_j\right)^2 + \mu\left(t_i - t_j\right)^2 \tag{6}$$

where μ is the scale factor of the temporal and spatial distance; then the GTWR model is built and compared with the other models (OLS, GWR, TWR, and GTWR) by a series of goodness-of-fit statistics, i.e., corrected Akaike Information Criterion (AICc) [29].

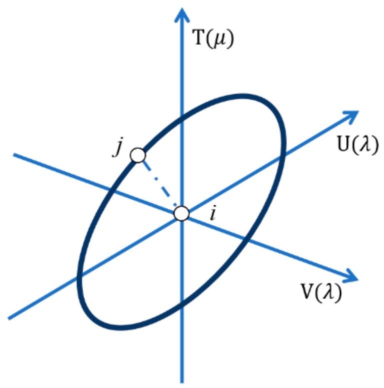

Figure 1. Schematic diagram of the spatio-temporal distance of the GTWR model.

3. Results and Discussions

3.1. Analysis of Spatio-Temporal Variation of NO_2 Pollution

Figure 2 presents the annual mean of NO_2 VCDs at the prefectural city level from 2005 to 2020. The most severe NO_2 pollution is mainly located in northern China during this sample period. Notably, we observe that some northern cities were highly polluted, for example, Jiaozuo (Henan Province), Handan (Hebei Province), Shijiazhuang (Hebei Province), and Xingtai (Hebei Province), in which NO_2 VCDs are larger than 2000×10^{13} molecule/cm^2. Apart from the North China Plain, moderately polluting cities (larger than 800×10^{13} molecule/cm^2) were observed in the important urban clusters, such as the Yangtze River Delta, Pearl River Delta, and Sichuan-Chongqing urban agglomeration.

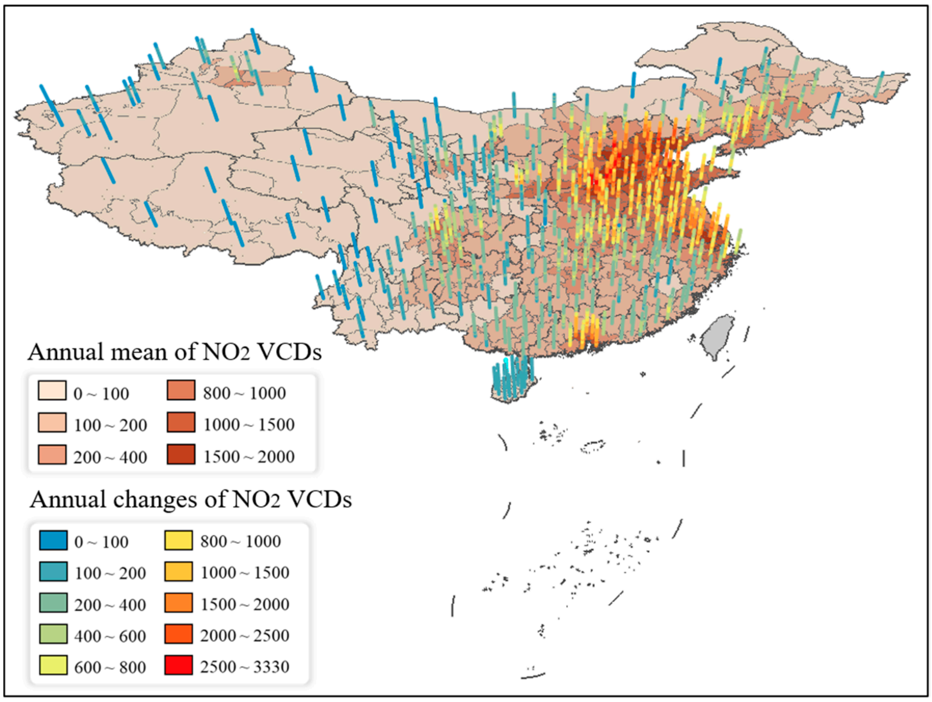

Figure 2. The annual mean of NO_2 VCDs and yearly changes of NO_2 VCDs from 2005 to 2020. (Unit: $\times 10^{13}$ molecule/cm^2).

The annual variations of NO_2 VCDs at the prefectural city levels can also be observed in Figure 2. It is widely known that the Chinese government usually sets pollutant reduction targets and measures in a series of Five-Year Plans. More specifically, NO_2 VCDs are closely synchronized with three Five-Year Plan periods in our study sample period, namely the 11th Five-Year Plan (2006–2010), 12th Five-Year Plan (2011–2015), and 13th Five-Year Plan (2016–2020). It can be observed that most cities increased the NO_2 pollution during the 11th Five-Year Plan, then began to decrease the NO_2 level during the 12th Five-Year Plan.

Figure 3 shows the percentage change of NO_2 VCDs during the three periods, namely between 2005 and 2019 (a), between 2005 and 2020 (b), and during the COVID-19 pandemic (c) in Chinese cities. We observed that NO_2 pollution in 130 cities in 2019, the end of the 13th Five-Year Plan (2016–2020), were lower than that in those cities in 2005. Most cities in the Yangtze River Delta and Pearl River Delta regions have seen a reduction in NO_2 VCDs by 10% or greater. Some cities in the southwest, however, have experienced a 10–30 percent increase in NO_2 levels. A total of 187 cities (about 56.0%) had lower NO_2 levels in 2020 than those in 2005. The rapid reduction of NO_2 levels implies that Chinese cities have effectively and efficiently implemented the NO_2 reduction strategies during the 13th Five-Year Plan.

Besides, to further evaluate the impact of the COVID-19 pandemic on NO_2 VCDs levels in prefecture-level cities, we compared the average values of February and March 2020 with the average values of earlier two years, namely, 2018 and 2019, removing the influence of the Chinese New Year on NO_2 levels. As shown in Figure 3c, we noticed that the COVID-19 pandemic resulted in a decrease in NO_2 in 288 (86.2%) Chinese cities. In particular, NO_2 VCDs significantly fell by more than 30 percent in some cities of the North China Plain and Yangtze River Delta regions. This shows that the epidemic has also exerted a significant impact on the traffic, industrial, and living activities in the local cities, leading to the rapid reduction of the NO_2 levels. Furthermore, the cities in the Pearl River Delta region are the exceptions, with NO_2 levels declining from 2005 to 2020 as a result of the Guangdong and Hong Kong governments' joint emissions control efforts, which began in 2003 [16].

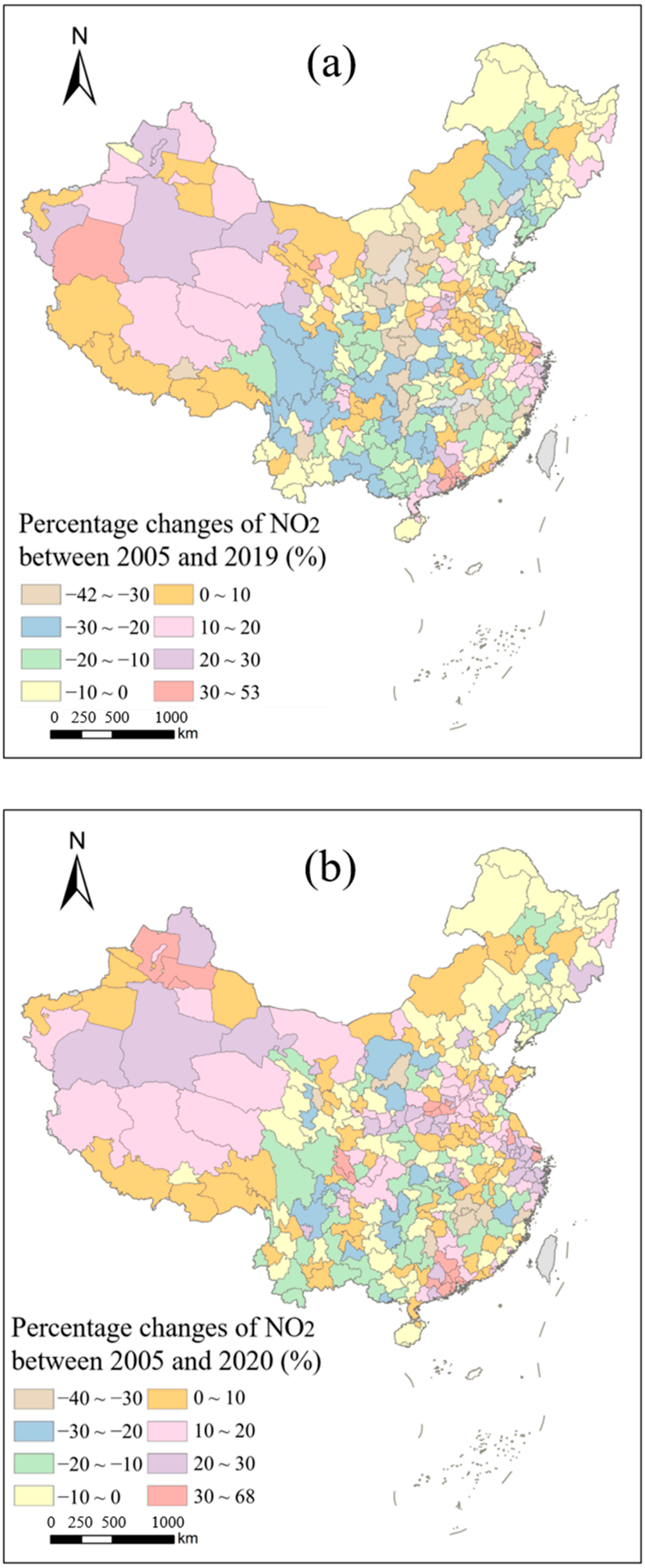

Figure 3. *Cont.*

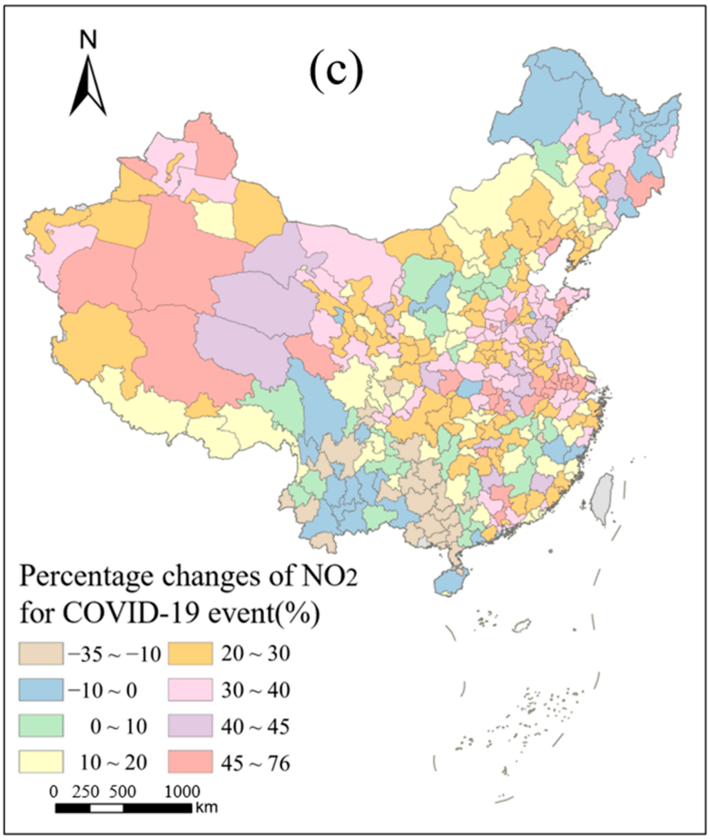

Figure 3. Percentage changes of NO_2, between 2005 and 2019 (**a**), between 2005 and 2020 (**b**), and during the COVID-19 pandemic (**c**).

A spatial autocorrelation among the NO_2 pollution of these Chinese cities can be verified. We then calculated the Moran's *I* value of annual mean NO_2 levels at the city level for robustness check using ArcGIS 10.8 software. As shown in Figure 4, the results indicated that the global Moran's *I* values during the sample period were statistically significant and larger than zero (p-value < 0.05 at the 95% confidence level), indicating that NO_2 pollution exhibits a significant positive spatial autocorrelation every year.

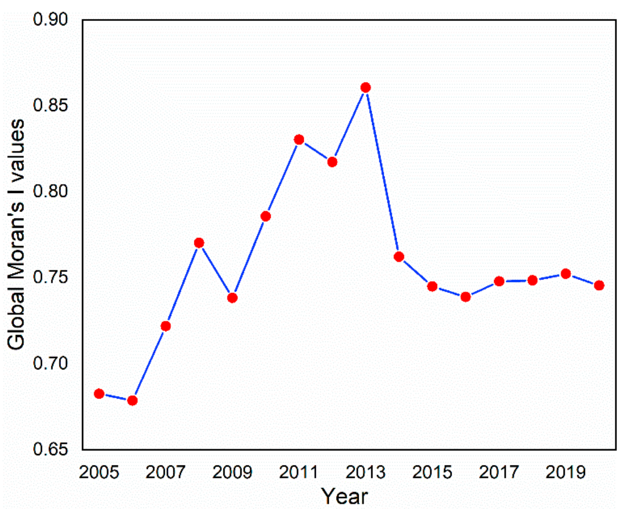

Figure 4. Global Moran's *I* values of NO_2 from 2005 to 2020.

Next, the local Moran's I in 2005, 2010, 2015, and 2020 were calculated. The LISA cluster maps in 2005, 2010, 2015, and 2020 (the end of each Five-Year Plan period) are depicted in Figure 5. It was discovered that the high–high cluster regions in these years were located in the North China Plain and the Yangtze River Delta. The high–high cluster of NO_2 pollution appeared in Pearl River Delta only in 2005. The low–low cluster regions of NO_2 pollution were mainly located in western China and northeastern China. Additionally, it is noted that the low–low cluster regions narrowed from 2005 to 2020.

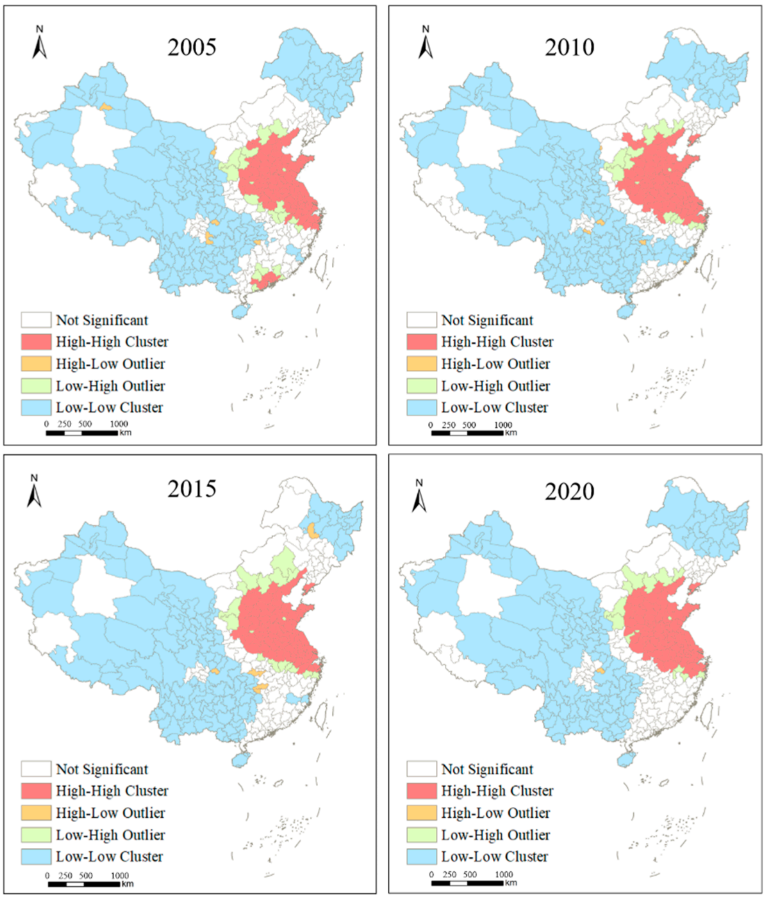

Figure 5. LISA cluster maps of annual mean NO_2 in 2005, 2010, 2015, and 2020.

3.2. Regression Results

We selected eight important socio-economic and natural independent variables for this study: namely, GDP per capita, population density, ratio of the tertiary to the secondary industry, foreign direct investment, temperature, wind, pressure, and humidity. The hypothesized spatio-temporal relationships between NO_2 pollution and the independent variables are demonstrated with an N*T estimated coefficient matrix. Otherwise, such variations may be averaged incorrectly in a global model (e.g., OLS). Hence, the GTWR is able to capture the spatio-temporal heterogeneous impacts of these explanatory variables locally on NO_2 pollution in each city.

Table 2 presents the estimation results of four models, namely, OLS, TWR, GWR, and GTWR. We find that the GTWR model has the highest R^2 value (0.904) compared with that of GWR (0.879), TWR (0.804), and OLS (0.776), indicating that the GTWR model has the highest explanatory power. Additionally, the GTWR model has the lowest AICc value (170.898) and the residual sum of squares (218.057) among these four models, also showing that the GTWR model is the best fitted compared to the other models in terms of these goodness-of-fit statistics. In general, the GTWR models might be suitable for analyzing n the spatial and temporal variations of the influencing factors of NO_2 pollution in this study.

Table 2. Comparison of the goodness of fit statistics for the four models.

	OLS	TWR	GWR	GTWR
Bandwidth		0.173	0.154	0.115
RSS	518.165	440.587	249.372	218.057
AICc	3229.014	2692.45	570.299	170.898
R^2	0.776	0.804	0.879	0.904
Adjusted R^2	0.774	0.803	0.877	0.903
Spatio-temporal Distance Ratio				0.373

Given the geographical disparities and temporal trends in NO_2 pollution, natural geographic conditions, and socio-economic factors prevalent in all Chinese prefecture-level cities, there are apparent spatial and temporal variances in the effects of each explanatory variable on NO_2 VCDs. As a result, the GTWR model was developed to examine the impacts of relevant factors on NO_2 pollution in each city at different times. Table 3 summarizes the descriptive statistics for the estimated coefficients of the GTWR model (i.e., mean, median, minimum (Min), and maximum (Max)).

Table 3. Descriptive statistics for GTWR regression coefficients of influencing factors.

Variable	Mean	Median	Min	Max
LnFDI	0.021	0.022	−0.022	0.072
LnPD	0.611	0.620	0.211	0.920
LnGDPPC	0.221	0.215	−0.143	0.532
LnTSRatio	−0.222	−0.220	−0.410	0.150
LnTemp	−1.094	−0.987	−3.484	2.557
LnPres	2.711	2.059	−1.945	9.210
LnWS	−0.191	−0.173	−2.918	1.328
LnHumi	−2.100	−2.387	−4.564	2.606
Intercept	−14.246	−10.576	−37.875	7.972

Overall, GDP per capita, population density, foreign direct investment, and air pressure are positively correlated with NO_2 pollution. In contrast, the ratio of the tertiary to the secondary industry, temperature, wind speed, and relative humidity are negatively correlated with NO_2 pollution. This means that the increases in GDP per capita, population density, and foreign direct investment exacerbate NO_2 pollution in most cities. A similar finding also applies to the air pressure variable. By contrast, increasing the ratio of the tertiary to the secondary industry or warmer, windier, or more humid climates could reduce NO_2 VCDs.

Figures 6 and 7 depict the temporal and spatial variations in the coefficients of the explanatory factors in the estimated results of the GTWR model from 2005 to 2019. As illustrated in Figure 6, most GDP per capita coefficients are positive, with only a few negative coefficients. GDP per capita is generally used to indicate the economic development level. It is linked because it generates a large amount of NO_2 emissions due to the raw economic development pattern typically adopted in the early period. Meanwhile, the GDP per capita coefficients in these cities from southern and northwestern China are the highest, indicating that increasing GDP per capita in these cities can increase NO_2 pollution dramatically. On the contrary, the northeastern and North China Plain cities have the lowest GDP per capita coefficients. We can conclude that the GDP per capita coefficients trend gets smaller as time increases from a temporal perspective. This reflects that the local economy has begun to intensify, allowing for a drop in NO_2 pollution per unit of GDP per capita.

All coefficients of the population density variable are observed to be positive. This is because the urban population growth will increase energy consumption, resulting in increased NO_2 emissions. As can be seen, population density expansion plays a crucial role in improving local NO_2 pollution in northern cities of China, notably in the northeast. The cities with the lowest coefficients, however, are located in southern and eastern China.

From a temporal perspective, the effect of population density on NO_2 pollution became stronger in the early study period and then turned smaller in most cities across the country, demonstrating that people have become more environmentally friendly and green in energy consumption in recent years.

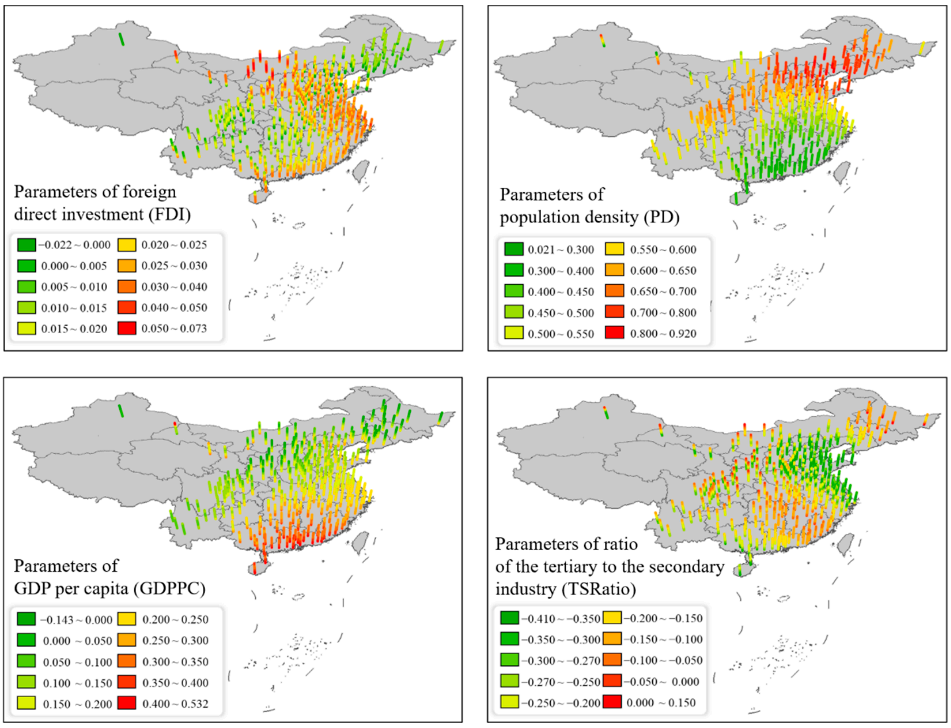

Figure 6. Spatio-temporal variations of the coefficients of socio-economic factors during 2005–2019 (from **bottom** to **top**).

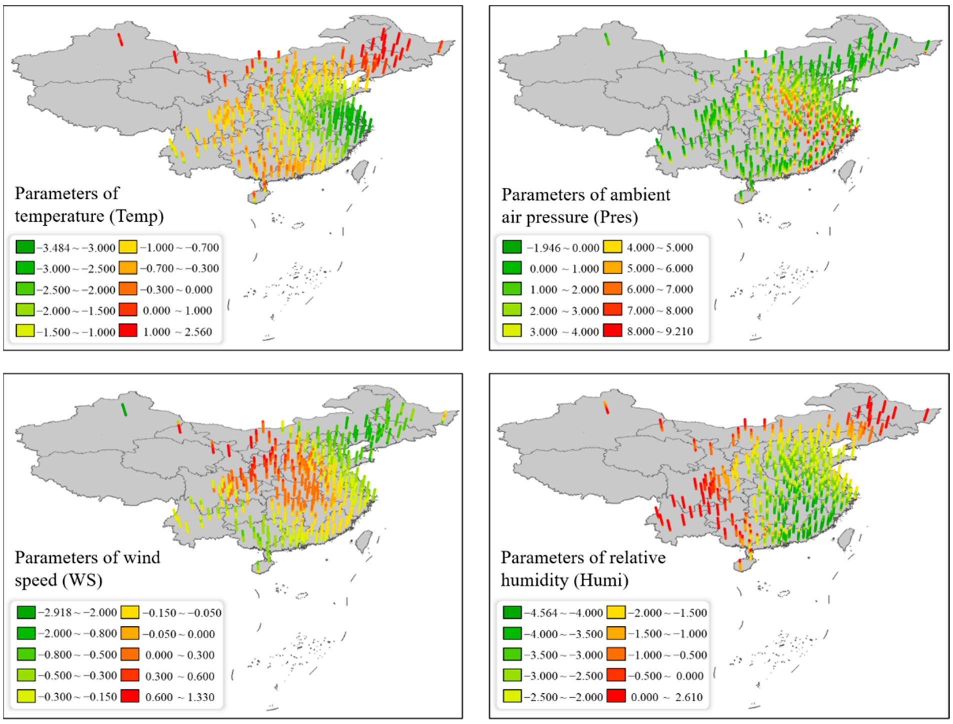

Figure 7. Spatio-temporal variations of the coefficients of metrological factors during 2005–2019 (from **bottom** to **top**).

Cities in northeastern China and northwestern China had the most significant TSRatio coefficients. The TSRatio variable of Hebei, Henan, Shandong, Jiangsu, Yunnan, Guangxi, and Hainan cities is negatively correlated and NO_2 pollution. NO_x emitted by the tertiary industry is mainly from service and transportation, and the industrial NO_x emission comes from the secondary industry. The negative coefficients suggest that increasing the shares of the tertiary industry may contribute to reducing NO_2 pollution. From a temporal view, we notice that the coefficients in eastern China and northeastern China decreased from 2005 to 2020. However, in western China and central China, their coefficients were increasing. We can infer that the contribution of services and transportation to NO_2 pollution is more significant than the increase in pollution levels caused by the secondary industry between 2005 and 2020. On the other hand, this also reflects that most cities in China have significantly improved their capacity to reduce industrial NO_x emissions in recent years.

Most positive coefficients of foreign direct investment are concentrated in eastern and central China. Since foreign direct investment can bring advanced technologies from industrialized countries, it can help improve urban air quality to a certain extent. However, the GTWR model results indicate that changes in foreign direct investment have a negligible influence on NO_2 pollution. Additionally, it can be observed from the time dimension perspective that the effect of foreign direct investment decreases with time for most cities.

As shown in Figure 7, meteorological variables, including temperature, ambient air pressure, wind speed, and relative humidity, are also strongly correlated with the tropospheric NO_2 VCDs in various cities. Generally, increasing temperature accelerates photochemical reactions and decreases the atmospheric lifetime of NO_2; increasing relative humidity reduces tropospheric NO_2 by increasing the rate of NO_x conversion to secondary aerosols; wind speed affects the rate of pollution diffusion and dilution in the atmosphere; and increasing air pressure increases NO_2 levels by improving atmospheric stability. From Figure 7, we find that the GTWR model results present a positive association between air pressure and NO_2. On the other hand, increasing temperature, wind speed, and humidity can help cities alleviate NO_2 pollution.

Additionally, we normalized each explanatory variable to examine the variable's contribution to NO_2 pollution. Table 4 summarizes the estimated coefficients for each explanatory variable after standardization. We compared the mean and median values of the variables' coefficients and discovered that population density had the highest positive coefficients, 0.609 (mean) and 0.611 (median). On the other hand, humidity has the most significant negative coefficients, −0.375 (mean) and −0.426 (median). As a result, we quantified the contribution of each variable to NO_2 pollution by ranking them according to the absolute magnitude of their coefficients: population density (0.609), humidity (−0.375), GDP per capita (0.210), air pressure (0.193), temperature (−0.189), the ratio of the tertiary to the secondary industry (−0.141), foreign investment (0.066), and wind speed (−0.058).

Table 4. Descriptive statistics for standardized coefficients of influencing factors.

Variable	Mean	Median	Min	Max
LnFDI	0.066	0.069	−0.070	0.228
LnPD	0.609	0.611	0.229	0.998
LnGDPPC	0.210	0.216	−0.686	0.769
LnTSRatio	−0.141	−0.139	−0.260	0.097
LnTemp	−0.189	−0.170	−0.601	0.437
LnPres	0.193	0.146	−0.138	0.999
LnWS	−0.058	−0.052	−0.882	0.401
LnHumi	−0.375	−0.426	−0.814	0.465

4. Conclusions

This study explored the spatial and temporal variations of NO_2 pollution in the prefecture-level city from 2005 to 2020, covering the 11th, 12th, and 13th Five-Year Plan periods. The most polluting cities were located in the North China Plain. NO_2 VCDs in more than half of cities in 2020 was lower than that in 2005. In addition, 86.2% of Chinese cities experienced a rapid reduction in the NO_2 VCDs in February and March of 2020 due to the COVID-19 pandemic. It indicates that both the NO_2 reduction strategies and the COVID-19 pandemic have led to the great NO_2 reduction in the 13th Five-Year Plan. The global Moran's *I* results suggested that NO_2 pollution in Chinese cities was highly spatially clustered. The local Moran's *I* results indicated that high–high NO_2 polluted cities were located in the North China Plain regions while the low–low cities were in western China and northeastern China.

Meanwhile, the results obtained from the GTWR model analysis allow us to bring the following policy insights. First, the high-density population in cities is not conducive to reducing NO_2 pollution, especially in the cities in the northwest and northeast. Therefore, appropriate adjustment of population size can help reduce air pollution. Meanwhile, people need to be encouraged to use more clean energy and raise environmental awareness of energy-saving and conservation. Secondly, although GDP per capita is positively correlated with NO_2 pollution, the coefficient of GDP per capita has been gradually decreasing in recent years, indicating that NO_2 pollution gradually starts to reduce as income increases. Finally, if the ratio of the tertiary to the secondary industry increases, it can effectively reduce NO_2 pollution, especially in the North China Plain and the Yangtze River Delta. It can achieve a good effect on alleviating air pollution.

However, this study still has limitations that can be solved in future work. For example, the satellite observed NO_2 data used in this study are the tropospheric NO_2 vertical column densities products, which have a certain non-linear relationship with the ground-level NO_2 concentrations. Future work needs to transform tropospheric NO_2 column concentrations to ground-level NO_2 concentrations with some specific technical means for further analyses and discussions. In addition, more accurate socio-economic data could be used to replace the data from traditional yearbooks.

Author Contributions: Conceptualization, Y.C. and L.J.; Data curation, H.Z. and Q.H.; Methodology, L.J. and Y.C.; Visualization, H.Z. and Y.C.; Writing—original draft and formal analysis, Y.C. and L.J.; Writing—review and editing, L.J. and Y.D.; resources, Y.D. and L.Q. All authors have read and agreed to the published version of the manuscript.

Funding: This research was funded by the Humanities and Social Science project of Ministry of Education of China (20YJCZH014), the National Natural Science Foundation of China (42101326), the Fundamental Research Funds for the Central Universities (B220201008), the project(C) of Qianjiang Talent Plan of Zhejiang Province, China (QJC1902005), and the Postdoctoral Fund of China (2021M703298).

Data Availability Statement: Not applicable.

Conflicts of Interest: The authors declare no conflict of interest.

References

1. Richter, A.; Burrows, J.P.; Nusz, H.; Granier, C.; Niemeier, U. Increase in tropospheric nitrogen dioxide over China observed from space. *Nature* **2005**, *437*, 129–132. [CrossRef] [PubMed]
2. Cooper, M.J.; Martin, R.V.; Hammer, M.S.; Levelt, P.F.; Veefkind, P.; Lamsal, L.N.; Krotkov, N.A.; Brook, J.R.; McLinden, C.A. Global fine-scale changes in ambient NO_2 during COVID-19 lockdowns. *Nature* **2022**, *601*, 380–387. [CrossRef] [PubMed]
3. Cui, Y.; Zhang, W.; Bao, H.; Wang, C.; Cai, W.; Yu, J.; Streets, D.G. Spatiotemporal dynamics of nitrogen dioxide pollution and urban development: Satellite observations over China, 2005–2016. *Resour. Conserv. Recycl.* **2019**, *142*, 59–68. [CrossRef]
4. Huang, S.; Li, H.; Wang, M.; Qian, Y.; Steenland, K.; Caudle, W.M.; Liu, Y.; Sarnat, J.; Papatheodorou, S.; Shi, L. Long-term exposure to nitrogen dioxide and mortality: A systematic review and meta-analysis. *Sci. Total Environ.* **2021**, *776*, 145968. [CrossRef]
5. Zhang, Q.; Geng, G.; Wang, S.; Richter, A.; He, K.B. Satellite remote sensing of changes in NO_x emissions over China during 1996–2010. *Chin. Sci. Bull.* **2012**, *57*, 2857–2864. [CrossRef]
6. Li, K.; Jacob, D.J.; Liao, H.; Zhu, J.; Shah, V.; Shen, L.; Bates, K.H.; Zhang, Q.; Zhai, S. A two-pollutant strategy for improving ozone and particulate air quality in China. *Nat. Geosci.* **2019**, *12*, 906–910. [CrossRef]
7. United Nations. *Transforming Our World: The 2030 Agenda for Sustainable Development*; United Nations: New York, NY, USA, 2015.

8. Persello, C.; Wegner, J.D.; Hansch, R.; Tuia, D.; Ghamisi, P.; Koeva, M.; Camps-Valls, G. Deep Learning and Earth Observation to Support the Sustainable Development Goals: Current Approaches, Open Challenges, and Future Opportunities. *IEEE Geosci. Remote Sens. Mag.* **2022**, *10*, 172–200. [CrossRef]
9. Fu, B.; Wang, S.; Zhang, J.; Hou, Z.; Li, J. Unravelling the complexity in achieving the 17 sustainable-development goals. *Natl. Sci. Rev.* **2019**, *6*, 386–388. [CrossRef]
10. Streets, D.G.; Canty, T.; Carmichael, G.R.; de Foy, B.; Dickerson, R.R.; Duncan, B.N.; Edwards, D.P.; Haynes, J.A.; Henze, D.K.; Houyoux, M.R.; et al. Emissions estimation from satellite retrievals: A review of current capability. *Atmos. Environ.* **2013**, *77*, 1011–1042. [CrossRef]
11. Zhang, L.; Lee, C.S.; Zhang, R.; Chen, L. Spatial and temporal evaluation of long term trend (2005–2014) of OMI retrieved NO_2 and SO_2 concentrations in Henan Province, China. *Atmos. Environ.* **2017**, *154*, 151–166. [CrossRef]
12. Cui, Y.; Jiang, L.; Zhang, W.; Bao, H.; Geng, B.; He, Q.; Zhang, L.; Streets, D.G. Evaluation of China's Environmental Pressures Based on Satellite NO_2 Observation and the Extended STIRPAT Model. *Int. J. Environ. Res. Public Health* **2019**, *16*, 1487. [CrossRef] [PubMed]
13. Zhang, Q.; Zheng, Y.; Tong, D.; Shao, M.; Wang, S.; Zhang, Y.; Xu, X.; Wang, J.; He, H.; Liu, W.; et al. Drivers of improved $PM_{2.5}$ air quality in China from 2013 to 2017. *Proc. Natl. Acad. Sci. USA* **2019**, *116*, 24463–24469. [CrossRef] [PubMed]
14. Müller, I.; Erbertseder, T.; Taubenböck, H. Tropospheric NO_2: Explorative analyses of spatial variability and impact factors. *Remote Sens. Environ.* **2022**, *270*, 112839. [CrossRef]
15. Wang, C.; Wang, T.; Wang, P. The Spatial–Temporal Variation of Tropospheric NO_2 over China during 2005 to 2018. *Atmosphere* **2019**, *10*, 444. [CrossRef]
16. Huang, J.; Zhou, C.; Lee, X.; Bao, Y.; Zhao, X.; Fung, J.; Richter, A.; Liu, X.; Zheng, Y. The effects of rapid urbanization on the levels in tropospheric nitrogen dioxide and ozone over East China. *Atmos. Environ.* **2013**, *77*, 558–567. [CrossRef]
17. Bucsela, E.J.; Krotkov, N.A.; Celarier, E.A.; Lamsal, L.N.; Swartz, W.H.; Bhartia, P.K.; Boersma, K.F.; Veefkind, J.P.; Gleason, J.F.; Pickering, K.E. A new stratospheric and tropospheric NO_2 retrieval algorithm for nadir-viewing satellite instruments: Applications to OMI. *Atmos. Meas. Tech.* **2013**, *6*, 2607–2626. [CrossRef]
18. Lin, J.T.; McElroy, M.B. Detection from space of a reduction in anthropogenic emissions of nitrogen oxides during the Chinese economic downturn. *Atmos. Chem. Phys.* **2011**, *11*, 8171–8188. [CrossRef]
19. Bichler, R.; Bittner, M. Comparison between economic growth and satellite-based measurements of NO_2 pollution over northern Italy. *Atmos. Environ.* **2022**, *272*, 118948. [CrossRef]
20. Mijling, B.; van der, A.R.J.; Boersma, K.F.; Van Roozendael, M.; De Smedt, I.; Kelder, H.M. Reductions of NO_2 detected from space during the 2008 Beijing Olympic Games. *Geophys. Res. Lett.* **2009**, *36*, L13801. [CrossRef]
21. Wang, Y.; Liao, H. Effect of emission control measures on ozone concentrations in Hangzhou during G20 meeting in 2016. *Chemosphere* **2020**, *261*, 127729. [CrossRef]
22. Feng, S.; Jiang, F.; Wang, H.; Wang, H.; Ju, W.; Shen, Y.; Zheng, Y.; Wu, Z.; Ding, A. NO_x Emission Changes Over China During the COVID-19 Epidemic Inferred from Surface NO_2 Observations. *Geophys. Res. Lett.* **2020**, *47*, e2020GL090080. [CrossRef] [PubMed]
23. Cao, H.; Han, L. The short-term impact of the COVID-19 epidemic on socioeconomic activities in China based on the OMI-NO_2 data. *Environ. Sci. Pollut. Res.* **2022**, *29*, 21682–21691. [CrossRef] [PubMed]
24. Luo, Z.; Xu, H.; Zhang, Z.; Zheng, S.; Liu, H. Year-round changes in tropospheric nitrogen dioxide caused by COVID-19 in China using satellite observation. *J. Environ. Sci.* **2022**, *in press*. [CrossRef]
25. Liu, Q.; Malarvizhi, A.S.; Liu, W.; Xu, H.; Harris, J.T.; Yang, J.; Duffy, D.Q.; Little, M.M.; Sha, D.; Lan, H.; et al. Spatiotemporal changes in global nitrogen dioxide emission due to COVID-19 mitigation policies. *Sci. Total Environ.* **2021**, *776*, 146027. [CrossRef]
26. Liu, F.; Zhang, Q.J.; van der, A.R.; Zheng, B.; Tong, D.; Yan, L.; Zheng, Y.; He, K. Recent reduction in NO_x emissions over China: Synthesis of satellite observations and emission inventories. *Environ. Res. Lett.* **2016**, *11*, 114002. [CrossRef]
27. Krotkov, N.A.; McLinden, C.A.; Li, C.; Lamsal, L.N.; Celarier, E.A.; Marchenko, S.V.; Swartz, W.H.; Bucsela, E.J.; Joiner, J.; Duncan, B.N.; et al. Aura OMI observations of regional SO_2 and NO_2 pollution changes from 2005 to 2015. *Atmos. Chem. Phys.* **2016**, *16*, 4605–4629. [CrossRef]
28. Cui, Y.; Lin, J.; Song, C.; Liu, M.; Yan, Y.; Xu, Y.; Huang, B. Rapid growth in nitrogen dioxide pollution over Western China, 2005–2013. *Atmos. Chem. Phys.* **2016**, *16*, 6207–6221. [CrossRef]
29. Huang, B.; Wu, B.; Barry, M. Geographically and temporally weighted regression for modeling spatio-temporal variation in house prices. *Int. J. Geogr. Inf. Sci.* **2010**, *24*, 383–401. [CrossRef]
30. Dong, F.; Li, J.; Zhang, S.; Wang, Y.; Sun, Z. Sensitivity analysis and spatial-temporal heterogeneity of CO_2 emission intensity: Evidence from China. *Resour. Conserv. Recycl.* **2019**, *150*, 104398. [CrossRef]
31. Li, T.; Shen, H.; Yuan, Q.; Zhang, L. Geographically and temporally weighted neural networks for satellite-based mapping of ground-level $PM_{2.5}$. *ISPRS J. Photogramm. Remote Sens.* **2020**, *167*, 178–188. [CrossRef]
32. Qin, K.; Rao, L.; Xu, J.; Bai, Y.; Zou, J.; Hao, N.; Li, S.; Yu, C. Estimating Ground Level NO_2 Concentrations over Central-Eastern China Using a Satellite-Based Geographically and Temporally Weighted Regression Model. *Remote Sens.* **2017**, *9*, 950. [CrossRef]
33. Wang, S.; Liu, Z.; Chen, Y.; Fang, C. Factors influencing ecosystem services in the Pearl River Delta, China: Spatiotemporal differentiation and varying importance. *Resour. Conserv. Recycl.* **2021**, *168*, 105477. [CrossRef]

34. Boersma, K.F.; Eskes, H.J.; Dirksen, R.J.; van der, A.R.J.; Veefkind, J.P.; Stammes, P.; Huijnen, V.; Kleipool, Q.L.; Sneep, M.; Claas, J.; et al. An improved tropospheric NO_2 column retrieval algorithm for the Ozone Monitoring Instrument. *Atmos. Meas. Tech.* **2011**, *4*, 1905–1928. [CrossRef]
35. Boersma, K.F.; Eskes, H.J.; Richter, A.; De Smedt, I.; Lorente, A.; Beirle, S.; van Geffen, J.H.G.M.; Zara, M.; Peters, E.; Van Roozendael, M.; et al. Improving algorithms and uncertainty estimates for satellite NO_2 retrievals: Results from the quality assurance for the essential climate variables (QA4ECV) project. *Atmos. Meas. Tech.* **2018**, *11*, 6651–6678. [CrossRef]
36. Anselin, L. Local Indicators of Spatial Association—LISA. *Geogr. Anal.* **1995**, *27*, 93–115. [CrossRef]
37. Wu, B.; Li, R.; Huang, B. A geographically and temporally weighted autoregressive model with application to housing prices. *Int. J. Geogr. Inf. Sci.* **2014**, *28*, 1186–1204. [CrossRef]
38. Bai, Y.; Wu, L.; Qin, K.; Zhang, Y.; Shen, Y.; Zhou, Y. A Geographically and Temporally Weighted Regression Model for Ground-Level $PM_{2.5}$ Estimation from Satellite-Derived 500 m Resolution AOD. *Remote Sens.* **2016**, *8*, 262. [CrossRef]